

X-RAY STUDY OF DISPERSIVENESS  
OF CADMIUM SULPHIDE-MANGANESE SULPHIDE SYSTEMS  
OBTAINED BY COPRECIPITATION\*

M. PAIĆ, K. KRANJC and V. PAIĆ

*Institute of Physics of the University of Zagreb, Zagreb*

Received 26 March 1971; revised manuscript received 3 June 1971

**Abstract:** The dispersiveness of CdS-MnS systems, obtained by coprecipitation from aqueous solutions of corresponding sulphates by  $(\text{NH}_4)_2\text{S}$ , was investigated by means of the broadening of Debye-Scherrer lines and small-angle X-ray scattering. An estimate of the size of crystallites was deduced from the half-width of a line in common to the hexagonal and cubic phases. The analysis of the small-angle scattering curves, applying two independent procedures, has given a consistent picture of the systems. The systems are granular, formed of approximately spherical particles. These often are clusters of as much as several hundreds of small crystallites. All parameters describing the systems show a remarkable dependence on the amount of MnS. In particular the parameters related to the size of the particles have a very pronounced maximum in the critical region of precipitation, where the amount of MnS is near 0.1 mol %. The specific surface has a minimum at the same value. The number of crystallites forming a particle diminishes abruptly in the critical region.

### *1. Introduction*

Intending to study the optical properties of CdS-MnS systems — obtained by precipitation from aqueous solutions — in correlation with the size of crystallites and particles, we investigated the broadening of their Debye-Scherrer lines and their small-angle X-ray scattering curves.

---

\* This work was supported by Federal Fund for Scientific Work.

## 2. Experimental

*Preparation of the systems.* The CdS-MnS systems were prepared by adding  $(\text{NH}_4)_2\text{S}$  to aqueous solutions of mixtures of  $\text{MnSO}_4$  and  $\text{CdSO}_4$  of various relative concentrations as described in detail by one of us<sup>1</sup>. The procedure of precipitation at 20 °C was exactly the same for all systems. Thus, each system is characterised by the relative concentration of  $\text{MnSO}_4$ ,  $p_{\text{MnSO}_4}$ , in the aqueous solution prior to precipitation and the amount of MnS,  $p_{\text{MnS}}$ , in the system. This amount is corrected for the quantity of water and excess sulphur which the systems may contain<sup>2</sup>. The corresponding pairs of values  $p_{\text{MnS}}$ ,  $p_{\text{MnSO}_4}$  give a characteristic function<sup>1</sup>,  $p_{\text{MnSO}_4} = g(\log p_{\text{MnS}})$ , to which we shall refer frequently in this paper. We prepared eleven systems each of which corresponds to one point on the characteristic function, marked by a capital letter. All measurements were made on samples which were not submitted to any heat treatment. They were only dried for months over silicagel at room temperature.

*Powder diagrams.* To obtain satisfactory powder diagrams it was necessary to use the diffractographic method. The X-rays were monochromatized by reflection (Co K  $\alpha$  radiation,  $\lambda = 1.7902 \text{ \AA}$ ). The size of the crystallites was evaluated by means of the Scherrer formula<sup>3</sup>. As the systems consist of a mixture of hexagonal  $\alpha$ -phase and of cubic  $\beta$ -phase<sup>1</sup> the half-width was measured on the 220  $\beta$ -CdS line common to both phases ( $2\theta = 52^\circ$ ). The correction for the instrumental width was made by means of  $\alpha$ -CdS crystals ground to powder.

*Small-angle scattering curves.* The nickel-filtered copper radiation and a Kratky camera were used. The specimen, reduced to the powder by gentle grinding, was spread uniformly between two cellulose acetate foils. The scattering was registered by photographic films. The specimen to foil distance was 260 mm. It was not possible to obtain the complete scattering curve by microphotometering one single film. Therefore, four diagrams of each specimen were taken with increasing exposure times, and the scattering curves combined into one. In this way the influence of the short wave length part of the continuous spectrum was lowered.

## 3. Results

*Size of crystallites.* The crystallite sizes as obtained by our simple procedure are only crude estimates for following reasons:

- a part of line broadening may be due to the imperfections of the lattice, and
- the crystallites of the cubic and hexagonal phases may have different sizes and shapes, and the relative amount of both phases may vary from specimen to specimen.

Curve (I) in Fig. 1. represents the relative size,  $L_i/L_F$ , of the crystallites of the system  $i$  compared to the size  $L_F = 3.95$  nm of the system  $F$  vs  $\log p_{\text{MnS}}$ . The system  $F$  does not contain MnS detectable by chemical analysis. The function  $L_i/L_F = f(\log p_{\text{MnS}})$  passes through a pronounced maximum at

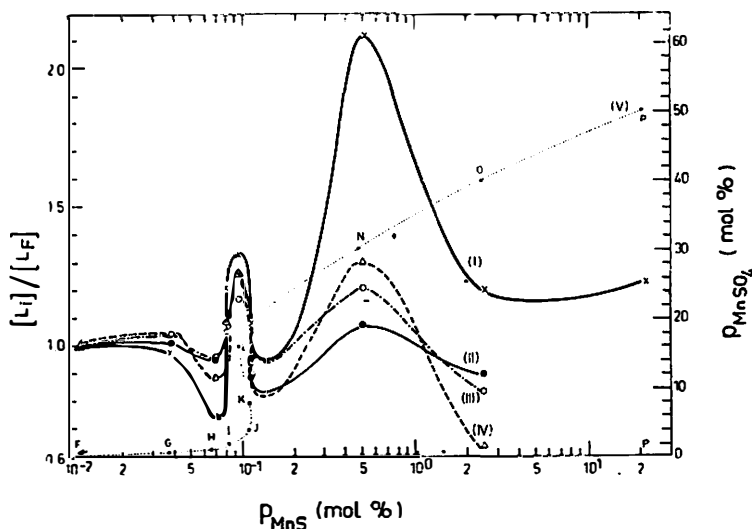


Fig. 1 — (I) relative size,  $L_i/L_F$ , ( $L_F = 3.95$  nm) of crystallites, derived from the width of the 220 line of the X-ray powder diagrams of the CdS-MnS systems, as a function of the logarithm of the molar content,  $p_{\text{MnS}}$ , in MnS. (II), relative mass average particle diameter,  $\langle 2R_i \rangle_m / \langle 2R_F \rangle_m$ , ( $\langle 2R_F \rangle_m = 29.2$  nm) and (III), relative number average particle diameter  $\langle 2R_i \rangle_n / \langle 2R_F \rangle_n$ , ( $\langle 2R_F \rangle_n = 11.4$  nm), derived from small-angle X-ray scattering by decomposing the scattered intensity in four Gaussian curves, as functions of  $\log p_{\text{MnS}}$ . (IV), relative statistical intercepts  $\bar{l}_i/\bar{l}_F$ , ( $\bar{l}_F = 12.2$  nm), derived from small-angle scattering, according to Porod's theory. (V),  $p_{\text{MnSO}_4} = g(\log p_{\text{MnS}})$  (right-hand ordinate); capital characters on this curve refer to the different systems studied in this and previous papers.

$p_{\text{MnS}} = 0.0954$  mol  $\%$ . The corresponding value of  $\Delta p_{\text{MnS}}$  is only about 0.04 mol  $\%$ . This maximum falls in the so-called critical region of precipitation marked by an approximately constant content of about 0.1 mol  $\%$  MnS. This region is characterised by a notable interval of concentration of  $\text{MnSO}_4$  in the aqueous solutions, as shown by curve (V)<sup>1</sup>.

Another maximum appears at about 0.5 mol  $\%$  MnS (system  $N$ ), in which the crystallites are twice as large as those of the system  $F$ . It is evident that, owing to the lack of experimental points, the outline of this maximum is entirely tentative.

*Size of the particles*<sup>4</sup>). To obtain an insight in the size and character of the particles, we resolved the small-angle scattering curve into four Gaussian curves, each of which represents, in the Guinier approximation, one

group of particles of identical radii of gyration, scattering independently. By this means the »scattering equivalent« of the system<sup>5)</sup> is obtained. We make the simplest assumption that the particles are spherical. The mass fraction ( $m$ ) and the number fraction ( $n$ ) of each group were found from the intercepts of the straight lines with the ordinate in the Guinier plot of the slit — corrected scattering curves. The radii of the four groups as well as the corresponding fractions, owing to their mass or to their number in each system, are represented in Fig. 2. The solid line rectangles correspond to the mass fractions, the broken line rectangles to the number fractions. All radii of one group and the corresponding number fractions or mass fractions fit inside a given rectangle when all systems are taken into account.

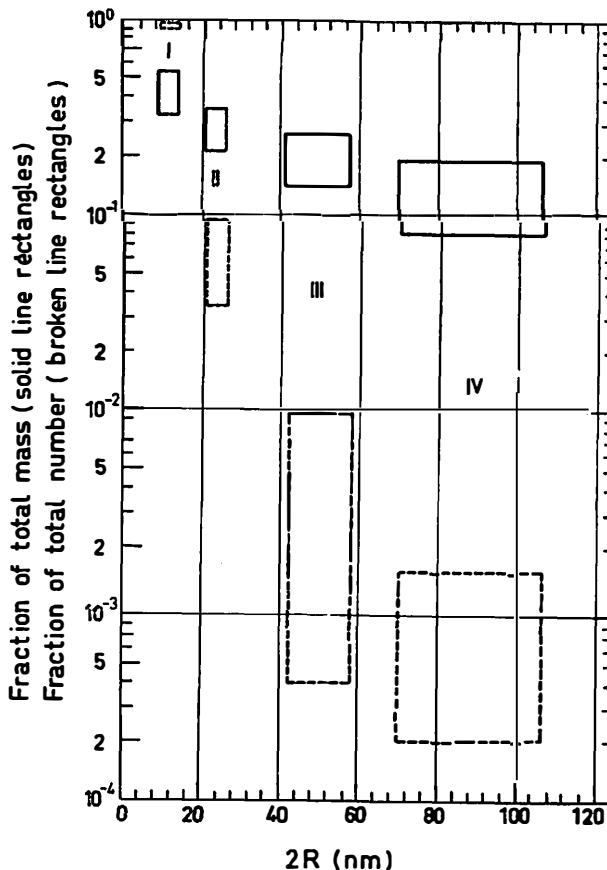


Fig. 2 — Logarithm of fractions of total mass (solid line rectangles) and logarithm of fractions of total number of particles (broken line rectangles) in which the systems can be split according to Gaussian analyses of the small-angle X-ray scattering, as functions of the diameter of the particles.

There is a very important number of small particles, more than 90% in group I, and a very small number of big particles, e. g. for the system *F* for which  $p_{MnSO_4} = 0$ ,  $p_{MnS} = 0$ ;  $2R_1 = 10.4$  nm,  $n_1 = 0.938$ ;  $2R_2 = 23.8$  nm,  $n_2 = 0.0558$ ;  $2R_3 = 49.0$  nm,  $n_3 = 0.00514$ ;  $2R_4 = 70.4$  nm,  $n_4 = 0.00083$ .

When the mass distribution is considered the fractions differ less, c. g. for the system  $F$ :  $m_1 = 0.392$ ;  $m_2 = 0.278$ ;  $m_3 = 0.222$ ;  $m_4 = 0.107$ .

In each group the radii depend on the content of MnS of the system, as shown in Fig. 3. The relative radii,  $R_i/R_F$  of the group of smallest particles (group I) show a slight maximum in the critical region, while the radii of the group of greatest particles (group IV) pass through a pronounced maximum.

The mass average radii and the number average radii can be deduced from these results. Curve (II), Fig. 1, shows the relative mass average particle diameter  $\langle 2R_i \rangle_m / \langle 2R_F \rangle_m$ , ( $\langle 2R_F \rangle_m = 29.2$  nm) as a function of  $\log p_{\text{MnS}}$ . Curve (III) on the same figure represents the relative number average particle diameter  $\langle 2R_i \rangle_n / \langle 2R_F \rangle_n$ , ( $\langle 2R_F \rangle_n = 11.4$  nm) as a function of the same variable. Both curves have marked maxima in the critical region and less pronounced maxima at  $p_{\text{MnS}} = 0.5$  mol %.

*Porod's parameters.* Applying Porod's general theory of small-angle scattering on a two-phase system with a well expressed boundary between the phases<sup>6, 7, 8</sup>, it is possible to deduce certain parameters describing the dispersiveness of the system, provided that the packing density  $p$  is known. To determine  $p$ , defined as the volume fraction of one phase, we used one sample which, after drying, conserved a geometrical form whose volume and mass could be measured. The average density of this sample was  $1.53$  g cm<sup>-3</sup>. As the true density of CdS is  $4.82$  g cm<sup>-3</sup> we have  $p = 1.53/4.82 = 0.317$  for this

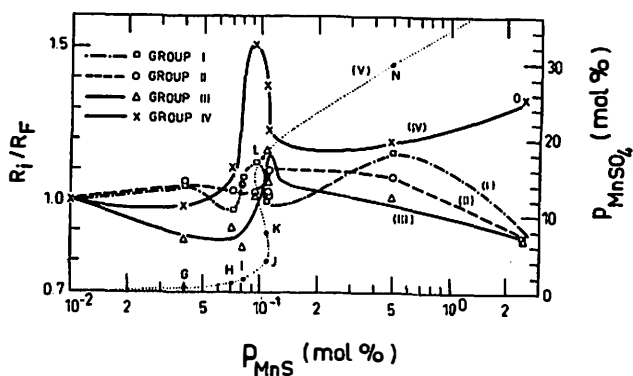


Fig. 3 — (I) to (IV), relative radii,  $R_i/R_F$ , of particles of a given group, represented in Fig. 2, as functions of  $\log p_{\text{MnS}}$ . (V),  $p_{\text{MnSO}_4} = g(\log p_{\text{MnS}})$ , (right-hand ordinate).

sample. We made the rather crude assumption ascribing to all our systems the same value of  $p$ . Adapting Porod's formulae to the infinite-slit collimated beam the following parameters were deduced.

*Specific surface.* This parameter is defined as the internal surface area  $S_{sp}$  per unit mass. In Fig. 4, curve (I) (triangles) shows the dependence of the relative specific surface  $S_{spi}/S_{spF}$ , ( $S_{spF} = 68$  m<sup>2</sup> g<sup>-1</sup>), on  $p_{\text{MnS}}$ . It is seen that this curve has two minima, one in the critical region, the other at 0.5 mol % MnS.

The specific surface can be calculated from the results of the Gaussian analysis (Fig. 2), under the assumption of spherical particles. In Fig. 4 these results are indicated by crosses. The concordance of the specific surfaces deduced from the scattering curves by two entirely different and independent procedures is striking. It enhances the confidence one may have in this kind of measurements. In the same figure we traced the relative water content,  $p_{H_2O i}/p_{H_2O F}$ , curve (II), ( $p_{H_2O F} = 1.4 \text{ mol } \%$ ) and the relative excess sulphur content  $p_{Si}/p_{SF}$ , curve (III), ( $p_{SF} = 2.7 \text{ wt } \%$ )<sup>2</sup>). Both curves show minima in the critical region, coinciding with the first minimum of the specific surface. The second minimum does not appear at  $0.5 \text{ mol } \%$  MnS but near  $2.5 \text{ mol } \%$  MnS. The first minimum of water content is much more pronounced than the minimum of sulphur content and the one deduced from the scattering curve. The minima of water and excess sulphur were interpreted as due to the minimum of the specific surface<sup>2</sup>).

*Intersects.* The specific surface is inversely proportional to a size parameter  $\bar{l}$  which is the number average value of all intersects occupied by the matter on the straight lines drawn through the specimen in all directions. The relative values  $\bar{l}_i/\bar{l}_F$ , ( $\bar{l}_F = 12.2 \text{ nm}$ ) of intersects as a function of  $\log p_{MnS}$  are shown by the curve (IV) in Fig. 1. This curve has all the features of the other curves in the same figure.

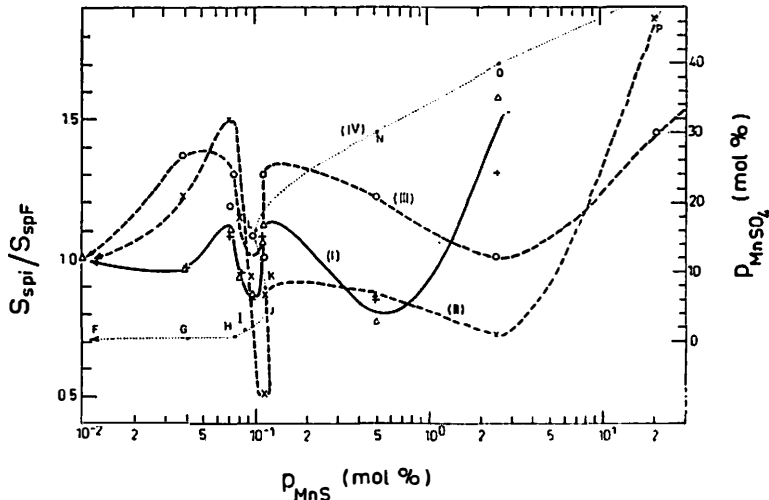


Fig. 4 — (I), relative specific surfaces  $S_{spi}/S_{spF}$ , ( $S_{spF} = 68.0 \text{ m}^2 \text{ g}^{-1}$ ) obtained by Porod's theory (triangles) and by Gaussian analyses (crosses), as functions of  $\log p_{MnS}$ . (II), relative content of water,  $p_{H_2O i}/p_{H_2O F}$ , ( $p_{H_2O F} = 1.4 \text{ wt } \%$ ) and (III), of sulphur,  $p_{Si}/p_{SF}$ , ( $p_{SF} = 2.7 \text{ wt } \%$ ), as functions of  $\log p_{MnS}$ . (IV),  $p_{MnSO_4} = (\log p_{MnS})$ , (right-hand ordinate).

*Reduced length.* Supposing equal packing density for all systems, the reduced length  $l_r$  is proportional to the intersect;  $l_r \equiv \bar{l}(l - p)$ . The corresponding values relative to the system  $F$  are thus identical to the relative values of the intersects, Fig. 1, curve (IV). We found for the system  $F$ ,  $l_{rF} = 8.33 \text{ nm}$ .

*Correlation length.* Independently of the parameters mentioned so far it is possible to deduce from the scattering curve the correlation length  $l_c$ . The relative values  $l_{ci}/l_{cF}$ , ( $l_{cF} = 19.4$  nm) as a function of  $\log p_{MnS}$  are given in Fig. 5, curve (I). To facilitate the comparison we reproduced in the same figure, curve (II) the relative reduced lengths  $l_{ri}/l_{rF}$ .

#### 4. Discussion

Porod has shown that small-angle X-ray scattering gives the internal specific surface of dilute and dense systems. As we already mentioned, Porod's theory and Gaussian analysis gave in our case, for a given system, very similar results. It means that we are, very probably, not far from reality if we consider that the systems consist of individual particles approaching spherical shape. This is also supported by the comparison of Porod's parameters with the number average diameters deduced from Gaussian analysis. Indeed the mean intersect  $\bar{l}$  (number average), which is a purely geometrical entity<sup>9)</sup> is, for a dilute system of equal spheres

$$\frac{\bar{l}}{2R} = \frac{2}{3}. \quad (1)$$

In the case of the system *F* the so calculated diameter is 18.3 nm or 38% in excess of  $\langle 2R \rangle_{nF}$ . The correlation length  $l_c$  may be considered as the approximate number average diameter of the equivalent scattering system. In

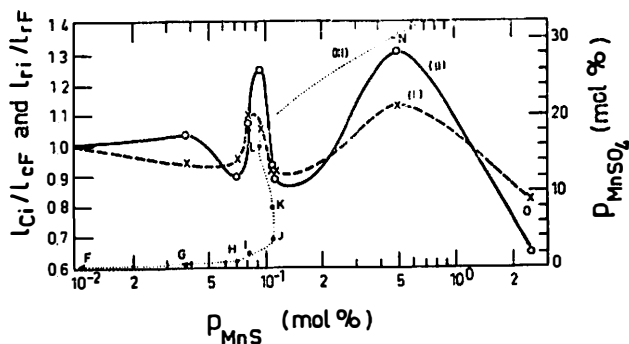


Fig. 5 — (I), relative correlation length  $l_{ci}/l_{cF}$ , ( $l_{cF} = 19.4$  nm) and (II), relative reduced length  $l_{ri}/l_{rF}$ , ( $2l_{rF} = 16.7$  nm) as functions of  $\log p_{MnS}$ . (III),  $p_{MnSO_4} = g(\log p_{MnS})$ , (right-hand ordinate).

a dilute system of identical spheres,  $l_c$  equals 3/4 of the diameter. For the system *F* this diameter would be 25.8 nm or 56% greater than  $\langle 2R \rangle_{nF}$ . Considering the errors and uncertainties of this kind of measurements and the simplifying assumptions which were made, these results seem to be consistent with the ones expected for a system of quasi spherical particles. To find a mean value connected with the particle sizes of polydisperse systems,

which can be more strictly related to  $\bar{l}$  than in relation (1), we equaled Porod's expression for the specific surface with the one found for a system of spheres of various diameters. The result:

$$\bar{l} \left\langle \frac{1}{2R} \right\rangle_m = \frac{2}{3}, \quad (2)$$

reduces, for a monodisperse system, to relation (1). In the case of the system *F*,  $l = 12.2$  nm,  $\langle 1/2R \rangle_m = 0.0555$  nm<sup>-1</sup> and their product is 0.677 or 1.5% in excess of 2/3. For our other systems this product differs from 2 to 12% from 2/3.

The correlation length depends not only on the size and shape of particles but also on their clustering. To characterise a given system, Porod introduces structural numbers, for example the dimension free ratio  $f = l_c/2l_r$ . For a dilute system of identical spheres  $f$  is about 1/2. Unfortunately the interpretation of the scattering curve is not unambiguous. So the structural number depends on formation of clusters, polydispersity and deviation from the spherical shape. It gives only general hints about what the structure

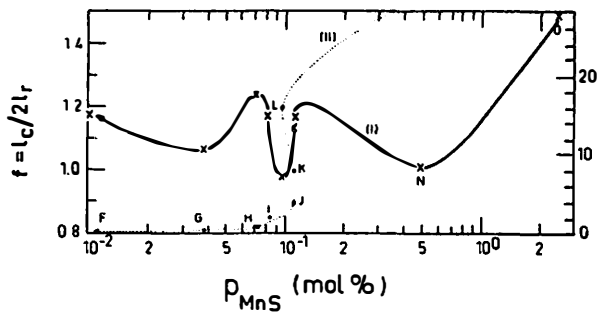


Fig. 6 — (I), structural number,  $f = l_c/2l_r$ , as a function of  $\log p_{MnS}$ . (II),  $p_{MnSO_4} = g(\log p_{MnS})$ , (right-hand ordinate).

of the system may be. In the case of the sample *F* the structural number is 1.17, a value indicating the possibility of a granular system. The structural number may be more useful for comparison of characteristics of similar systems as are the ones we have studied. Fig. 6 shows that for these systems  $f$  depends on  $p_{MnS}$  in a remarkable way. It has three minima and two relative maxima on each side of the minimum in the critical region. For all our systems the values of  $f$  do not much exceed 1, so all of them have the granular structure expected for precipitates. One may ask if the two maxima of  $f$  on either side of the minimum in the critical region indicate the same character of the systems, or if they have different origins. In fact an increase in  $f$  may be caused by formation of clusters, increase in polydispersity or deviation from sphericity, but the analysis of the scattering curves



alone can not decide between these possibilities. That is why we decided to measure the size of the crystallites.

The definition of a crystallite relevant in the analysis of the width of Debye-Scherrer lines differs from the definition of a particle in the evaluation of small-angle scattering. A particle can be polycrystalline, formed of clusters of many crystallites, or it may be amorphous, but it is defined as a volume of homogeneous electron density<sup>9</sup>. Under the assumption of perfect lattice of the crystallites, the ratio of the average volume of the supposedly spherical particles and the average volume of the supposedly cubic crystallites,  $(4/3) \langle R \rangle_{mi}^3 \pi / L_i^3 \approx 4 \langle R \rangle_{mi}^3 / L_i^3$ , may give an information on the number of crystallites clustering to form a particle. The functional dependence of this quantity on  $\log p_{MnS}$  (Fig. 7) is very different from the dependence of  $f$  on  $\log p_{MnS}$  (Fig. 6): it is asymmetric relative to the critical region and the maximum at higher values of  $p_{MnS}$  has disappeared. A mass average particle of the system *F*, under the simplifying assumptions we made, is a cluster of about 200 crystallites. As  $p_{MnS}$  increases towards the critical region, more crystallites cluster together to form larger particles. The maximum (450 crystallites) is reached for the system *H* ( $p_{MnS} = 0.0721$  mol %). In the critical

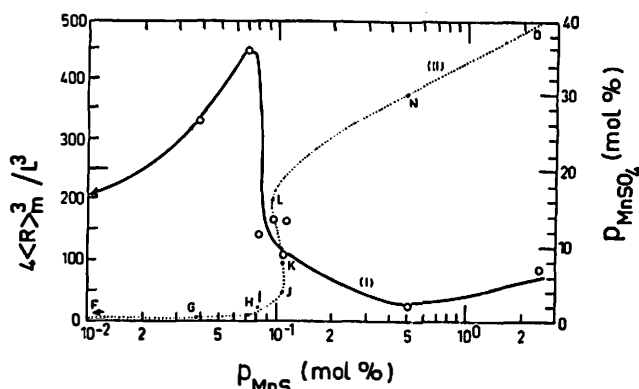


Fig. 7 — (I),  $8 \langle R \rangle^3 / L^3$  as a function of  $\log p_{MnS}$ . (II),  $p_{MnSO_4} = g(\log p_{MnS})$ , (right-hand ordinate).

region the particles are formed of a smaller number, about 150, of bigger crystallites. This tendency continues as  $p_{MnS}$  increases so that at  $p_{MnS} = 0.5$  mol % the number of crystallites per particle is only 25. Owing to these considerations the origin of the asymmetry of the function on Fig. 7 is the clustering of the crystallites.

### 5. Conclusions

The specific internal surface of our system is rather large ( $S_{spF} = 68.0$   $m^2 g^{-1}$ ) compared to typically very dispersed substances such as naphthalene soot ( $S_{sp} = 27.5$   $m^2 g^{-1}$ )<sup>9</sup>. It shows characteristic variations with the content

of MnS, particularly a minimum in the critical region of precipitation where the system contains 0.0954 mol % MnS. This minimum which, in our opinion, separates the precipitation of the saturated CdS-MnS solid solution from the exprecipitation with MnS, coincides with the minimum of water and excess sulphur content reported previously<sup>2)</sup>.

The analysis of small-angle scattering curves shows that the CdS-MnS systems are granular. This conclusion is supported by electron micrographs as the one of system *F* shown in Fig. 8. The dimension of particles depends characteristically on the content of MnS in the system which is a function of the relative concentration of the sulfates  $\text{CdSO}_4 + \text{MnSO}_4$ , prior to the precipitation. A remarkable relative maximum of the particle size is evident in the critical region of precipitation. The particles are mostly clusters of

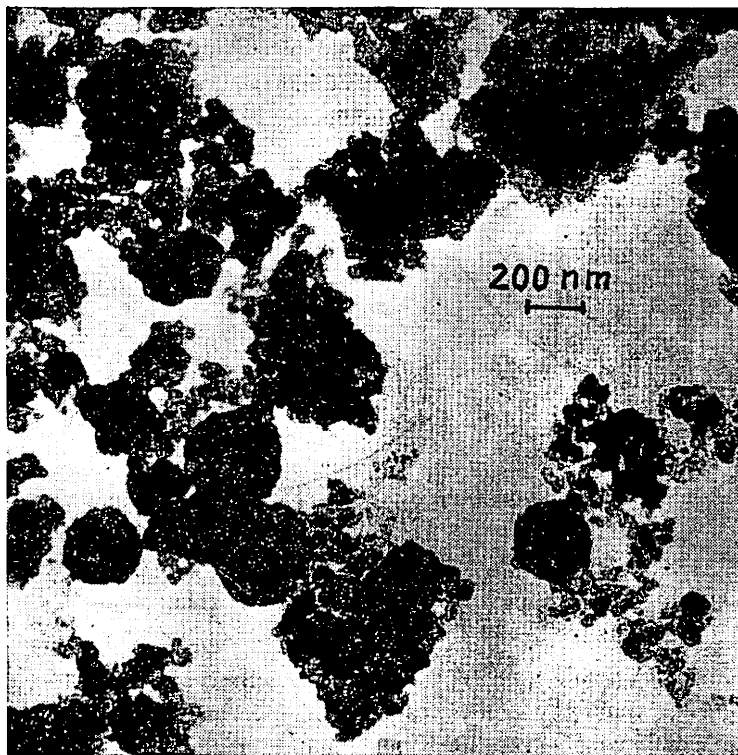


Fig. 8 — Electron micrograph of a sample of the system *F*.

numerous crystallites the size and number of which change across the critical region: the number of crystallites increases with the content of MnS up to the value of 0.07 mol % and then diminishes abruptly.

The systems are polydisperse, formed of a great number of small particles, approximately spherical in shape, and of a small number of large particles.

The particle diameters vary from about 10 nm to about 80 to 100 nm, the dimensions of the crystallites being from about 3 to 8 nm. The electron micrographs confirm the polydispersity of the systems without enabling extensive and significant measurements as the ones obtained by X-ray interference methods.

### *Acknowledgement*

The authors thank Mr. D. Kunstelj for the electron micrographs of several samples of the systems as well as Mr. V. Petrović for his valuable technical assistance.

### R e f e r e n c e s

- 1) M. Paić, *Croat. Chem. Acta*, **43**, (1971);
- 2) M. Paić and Z. Despotović, *Croat. Chem. Acta*, **43**, (1971);
- 3) See for example: A. Guinier, *Théorie et technique de la radiocristallographie*, Dunod, Paris 1956, p. 464;
- 4) K. Kranjc and M. Paić, *II Int. Conf. on Small-Angle X-ray Scattering*, Graz, August 1970;
- 5) M. H. Jelinek, E. Solomon and I. Fankuchen, *Ind. Eng. Chem. (Anal. Ed.)* **18**, (1946) 172;
- 6) L. Kahovec, G. Porod and H. Ruck, *Kolloid-Z.*, **133**, (1953) 16;
- 7) P. Mittelbach and G. Porod, *Kolloid-Z. u. Z. Polymere*, **202**, (1965) 40;
- 8) G. Porod, *Determination of General Parameters by Small-Angle X-Ray Scattering*, Proc. Conf. Small-Angle Scattering, Syracuse, 1965, Gordon and Breach, N. Y. p. 1;
- 9) See also: J. Méring and D. Tchoubar, *J. Appl. Cryst.* **1**, (1968) 153.

## RENDGENOGRAFSKO ISPITIVANJE DISPERZNOSTI SISTEMA KADMIJUM SULFID-MANGAN SULFID DOBIVENIH KOPRECIPITACIJOM

M. PAIĆ, K. KRANJC i V. PAIĆ

*Institut za fiziku Sveučilišta u Zagrebu*

### S a d r Ź a j

Disperznost CdS-MnS sistema, dobivenih koprecipitacijom iz vodenih otopina odgovarajućih sulfata pomoću  $(\text{NH}_4)_2\text{S}$ , ispitivana je pomoću proširenja Debye-Scherrer linija i raspršenja rentgenskih zraka pod malim kutem.

Veličina  $L$  kristalita nađena je iz poluširine zajedničke linije heksagonalnog  $\alpha$ -CdS i kubičnog  $\beta$ -CdS. Pod pretpostavkom da su čestice sferične, Gaussov-

ska analiza krivulja raspršenja pod malim kutem daje četiri grupe čestica, odgovarajućih radijusa  $R$ .

Porodova teorija dala je specifične površine  $S_{sp}$ , segmente  $\bar{l}$ , dužine korelacije  $l_c$ , reducirane dužine  $l_r$  i strukturni broj  $f$ . Za čisti CdS sistem nađeno je:  $L = 3.95$  nm;  $2R_1 = 10.4$  nm;  $2R_2 = 23.8$  nm;  $2R_3 = 49$  nm;  $2R_4 = 70.4$  nm (za svaki sistem određen je i srednji numerički odnosno maseni polumjer);  $S_{sp} = 68$  m<sup>2</sup> g<sup>-1</sup>;  $l = 12.2$  nm;  $l_r = 8.33$  nm;  $l_c = 19.4$  nm i  $f = 1.17$ .

Osim toga određen je i produkt  $l/\langle 1/2R \rangle_m = 0.675$ . Svi parametri veličine čestica upućuju na zrnatost sistema, sastavljenih od približno sferičnih čestica koje su često i nakupine od više stotina kristalita. Veličina parametara ovisi o količini MnS u sistemu. Napose, svi parametri koji se odnose na veličinu čestica prolaze izrazitim maksimumom u kritičnom području precipitacije u kojem je količina MnS u sistemima približno 0.1 mol %. Specifična površina ima minimum kod iste vrijednosti. Broj kristalita koji tvori česticu naglo se smanjuje u kritičnom području.